Experimental investigation on the hygrothermal behavior of a new multilayer building envelope integrating PCM with bio-based material

Dongxia Wu, Mourad Rahim, Mohammed El Ganaoui, Rabah Djedjig, Rachid Bennacer, Bin Liu

Experimental investigation on the hygrothermal behavior of a new multilayer building envelope integrating PCM with bio-based material

Dongxia Wu[a]; Mourad Rahim[a]; Mohammed El Ganaoui [a, *]; Rabah Djedjig[a]; Rachid Bennacer[b]; Bin Liu[c]

a. University of Lorraine, LERMAB, IUT H Poincaré de Longwy, 168 Rue de Lorraine. Cosnes et Romain, 54400 Longwy, France

b. University of Paris-Saclay, ENS Paris-Saclay, CNRS, LMT -, 91190, Gif-sur-Yvette, France

c. Tianjin Key Laboratory of Refrigeration Technology, Tianjin University of Commerce, Tianjin 300134, China

* Corresponding author: mohammed.el-ganaoui@univ-lorraine.fr

Present/permanent address: IUT Henri Poincaré de Longwy. 168 Rue de Lorraine. Cosnes et Romain, 54400 Longwy, France

Abstract

Bio-based materials have strong hygrothermal behavior and phase change materials (PCMs) have high thermal inertia, but they have usually been studied separately in most research. In this paper, the hygrothermal behavior of a multilayer building envelope integrating hemp lime concrete (HLC) and PCM was investigated at experimental level. The envelope was flanked by a climate chamber and the laboratory ambient to imitate the outdoor and indoor environments, respectively. Four envelope configurations comprising a reference (without PCM) and three configurations with PCM (PCM placed on the outdoor and indoor side, in the middle of the envelope) were considered in order to

study the effect of PCM and its position on the hygrothermal behavior of the envelope. The results showed that the PCM had a significant effect on the hygrothermal behavior of HLC, based on the high coupling between temperature and relative humidity. The characteristic time was considered to quantitatively evaluate temperature and relative humidity trends, and their value was increased with the participation of PCM. Moreover, PCM increased the heat store/release capacity linearly with its position. The closer the PCM was to the outdoor, the higher the heat store/release capacity and the lower the heating/cooling load from the envelope to the indoor environment. These phenomena were closely related to the PCM's temperature distribution and its corresponding specific heat capacity. Therefore, due to the envelope's thermal and hygric inertia on the indoor environment and the building's energy saving potential, it was recommended that the PCM be placed close to the outdoor side.

Keywords

Phase change material (PCM); Hemp lime concrete (HLC); Heat/moisture transfer; Hygrothermal behavior; Characteristic time; Heat store/release capacity.

1. Introduction

In the context of increasingly depleted non-renewable energy sources and high CO_2 emissions, the global energy system is set to be doubly challenged in the future: by the demand for more energy and less carbon [1]. However, as places where humans live, work, and play, buildings account for about 58% of energy consumption and 28% of CO_2 emission [2]. Moreover, people's requirements

as regards indoor comfort are increasing as society develops. Therefore, several technologies and solutions have been used to improve indoor comfort while saving energy and reducing CO2 emissions. The building envelope represents the boundary between interior and exterior, ensuring watertightness, insulation, air, and light circulation. With growing environmental concerns, building envelopes are called upon to participate in energy consumption regulation. However, building envelopes are responsible for 51% of total energy consumption [3]; therefore, huge energy saving potential can be achieved by optimizing them.

Temperature and relative humidity are two important parameters that affect indoor air quality and consequently occupants' heat and moisture comfort [4, 5]. It has been proved that inappropriate temperature and humidity leads to mold growth [6, 7], thereby affecting occupants' health and furniture's lifespan. Building envelope materials with excellent thermal and hygroscopic behavior are the solution to regulation of temperature and relative humidity. Bio-based materials and PCMs (phase change materials) seemed to be the answer to this question in the literature. Porous bio-based materials have moisture hygroscopic properties, while PCMs have thermal inertia properties. Also, CO_2 emissions are minimal during production and utilization of such materials [8-10].

Hemp concrete, as a bio-based material, can be used as a building envelope material. It has been recognized by many researchers due to its sustainability and interesting hygrothermal characteristics [11-13]. Compared with conventional building materials such as aerated concrete, it has low density and high porosity. Therefore, it has been extensively studied as a thermal insulating [14-16] and hygroscopic material [17-19] of building, which is beneficial for building energy saving [20-22]. Previous studies [23, 24] have proved the strong coupling between temperature and relative humidity

within HLC, and both of them affect the relative humidity change within the material. Besides, the hygric property is more sensitive to temperature change than relative humidity [25, 26]. Therefore, some researchers have studied the effect of temperature on hygroscopic behavior. Poyet et al. [27] presented the theoretical model based on the Clausius-Clapeyron equation and isosteric heat of sorption. Later, Colinart et al. [28, 29] verified it by hemp concrete experiments, and the results highlighted the temperature dependence on the adsorption curve. Rahim et al. [30] simulated the temperature dependency of the sorption curves of the hemp concrete envelope and found that the relative humidity behavior could be predicted accurately by taking into account the influence of temperature. Chennouf et al. [31] explored the effect of temperature on hygroscopic behavior by experiment and confirmed that the sorption-desorption process and moisture buffer value were highly affected by temperature. The researches above indicate the excellent hygrothermal behavior of hemp concrete and the importance of temperature.

PCM is also an envelope technology to maintain or provide thermal comfort in new buildings [32], and it provides enough thermal inertia to utilize the cold energy at night during the hottest time of the day [33-35]. A great deal of thermal energy is stored or released during the phase change process [36, 37]. In other applications of PCM, it behaves different when placed in different positions [38, 39]. Similarly, as part of the building envelope, its thermal behavior is different when placed in different positions [40]. The thermal performance of the building envelope when PCM was placed in different positions was studied by Jin et al. [41-44], who found that the state, heat flux, amplitude, and time delay were different according to the PCM's position. Besides, the optimal position of PCM changes with different influence factors such as thickness, heat fusion, and the

melting temperature of PCM. Lee et al. [45] studied the thermal behavior of PCM when placing it in the south and west walls at different positions in the envelope, and the results indicated that the optimal position of PCM in the south wall was closer to the outdoor environment compared to the west wall. Lagou et al. [46] analyzed the melting temperature and optimal positions of PCM in different European continent climatic conditions and found that all the optimal positions were located on the interior side but varied with the melting temperature. Fateh et al. [47, 48] concluded that the PCM was more active when it was placed in the middle position, which caused a 15% peak heat load reduction and obvious time delay. Similarly, the optimum position of PCM was also found to be located in the range between the middle and the external in some researches [49, 50]. Therefore, the different position of PCM in the envelope produces different thermal feedback and the determination of optimal position is significant.

According to the aforementioned literature, hemp concrete has excellent hygric inertia as an envelope to dampen ambient relative humidity changes. However, it has low thermal inertia because of its light weight. Also, temperature has a significant influence on relative humidity changes within hemp concrete. On the other hand, the high PCM thermal inertia can change the temperature field and dampen the temperature amplitude. Besides, the feedback benefit in terms of heat behavior from the PCM-based envelope depends on the PCM's position.

This research focuses on the hygrothermal behavior of the new building envelope integrating HLC (hemp lime concrete, one of the bio-based materials) and PCM at experimental level. This new envelope has both high thermal inertia and high hygric inertia. First, the hygrothermal properties of PCM and HLC were presented. Then, the experimental protocol was proposed. It was carried out by

connecting one side of the envelope to dynamic temperature and relative humidity changes provided by a climate chamber, which was used to imitate the outdoor environment. The other side was exposed to the laboratory ambient with relatively stable hygrothermal environment to imitate the indoor environment. Four combinations of temperature and relative humidity changes were set as boundary conditions in the climate chamber, including two identical and two opposite trends. Later, the hygrothermal behavior of the envelope using HLC only was analyzed and compared with three integrated envelopes combining HLC and PCM, which were distinguished by the different positions of PCM. The value, fluctuations, and differences between various points within the HLC were studied, temperature and relative humidity curves were quantitatively evaluated, and the impact of PCM and its position were analyzed. Finally, heat flux behavior was presented, the envelope's heating/cooling load and heat store/release capacity were calculated. The PCM's temperature distribution and specific heat capacity was investigated.

2. Materials and methods

2.1. Materials

The materials considered in this paper are HLC and PCM (Fig.1). The HLC sample was produced from lime binder, water, and hemp particles using the molding method. The finished HLC sample has high porosity, resulting in interesting thermal conductivity (0.12 W/(m·K)) and high water vapor permeability (2.23×10^{-11} kg/(m·s·Pa)) [30]. Therefore, it helps to weaken thermal transfer and regulate relative humidity as a building envelope material.

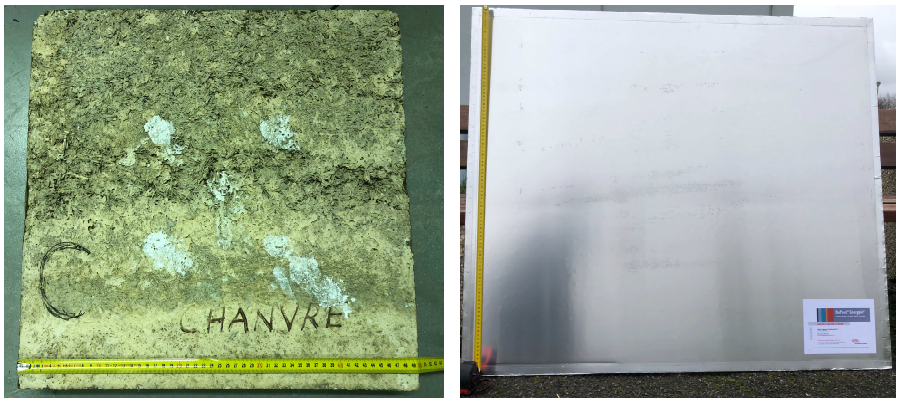

Fig. 1. Hemp lime concrete and phase change material

The PCM used in this paper is the finished panel called hydrocarbon-based PCM [52] (Dupont™ Energain®). It is comprised of ethylene-based polymer (40%) and paraffin wax (60%) laminated on both sides with a 0.1 mm aluminum sheet that ensures the paraffin's mechanical stability. The relation curve between the PCM's specific heat capacity and temperature is plotted in Fig.2. Distribution of the data follows a bell-shaped curve and maximum value is achieved at around 22 ℃. The melting process takes place between 10 and 28 ℃ with a sudden variation between 18 and 24 ℃, and latent heat is around 136.2 kJ/kg. Once the indoor temperature increases, it starts melting and absorbs thermal energy. Conversely, when the temperature drops, it solidifies and releases the absorbed energy.

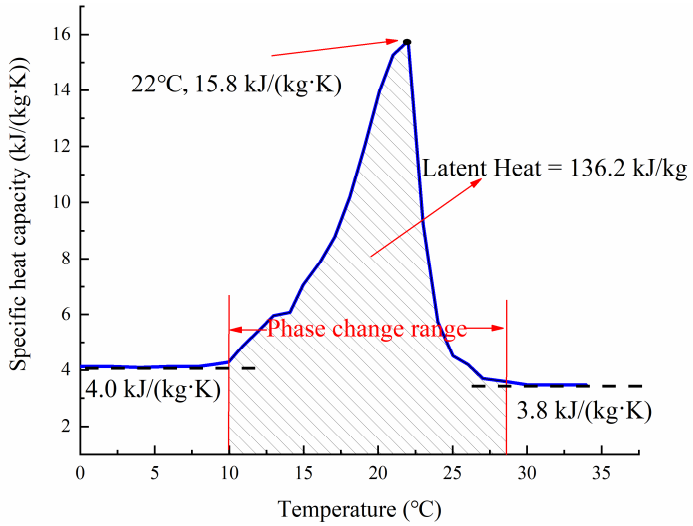

Fig. 2. Specific heat capacity of PCM [52]

Dimensions of each HCL and PCM were 50 cm × 50 cm × 7 cm and 50 cm × 50 cm × 2.12 cm respectively. Their basic physical parameters are summarized in Table 1.

Material	Density [kg/m^3]	Thermal conductivity [W/(m·K)]	Specific heat capacity [J/(kg·K)]	Water vapor permeability [kg/(m·s·Pa)]	Porosity [%]
HLC [30]	478	0.12	1100	2.23×10^{-11}	76.4
PCM [52]	810	Solid：0.18 Liquid: 0.14	Solid：4000 Liquid: 3800	—	—

Table 1 Basic physical and hygrothermal properties of HLC and PCM

2.2. Experimental protocol and monitoring points

Fig. 3 shows a schematic side view (a) and the actual experimental setup (b). One side surface of

the envelope was connected to the given environment provided by the climate chamber, while the other side surface was connected directly to the laboratory ambient. In order to ensure unidirectional transfer of heat and moisture through the envelope under study, the lateral surfaces were insulated with polyethylene film and polystyrene foam.

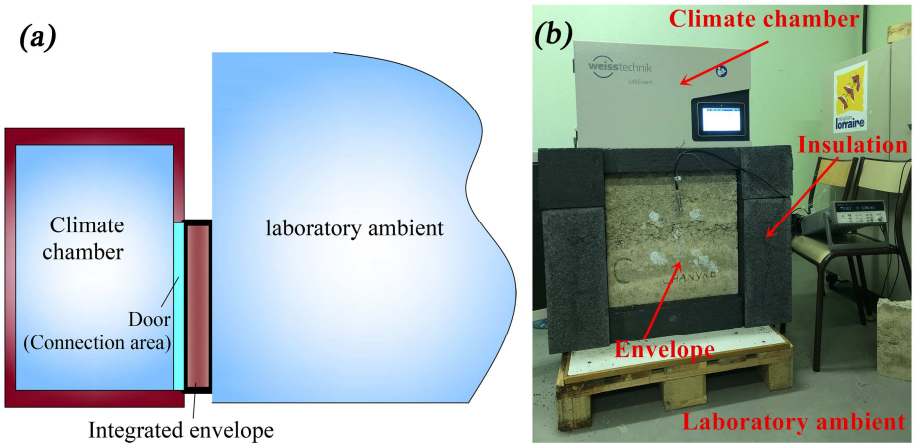

Fig. 3. (a) Sketch of the experimental setup; (b) Actual experimental setup

Two HLC layers and one PCM layer were used to test and compare the different configurations of the envelope composition under study. Four envelope configurations were considered according to the PCM's participation and its distance from the climate chamber. They are shown in Table 2 and Fig. 4(a), the climate chamber and laboratory ambient are located on the left and right side respectively.

Configurations (L: the thickness of HLC)	Multilayer from climate chamber to ambient	Total thickness [cm]

Without PCM	HLC + HLC	14
X=0 L (PCM on the climate chamber side)	PCM + HLC + HLC	16.12
X=0.5 L (PCM in the middle of HLCs)	HLC + PCM + HLC	16.12
X=1 L (PCM on the laboratory ambient side)	HLC + HLC + PCM	16.12

164 Table 2 Different envelope configurations

165

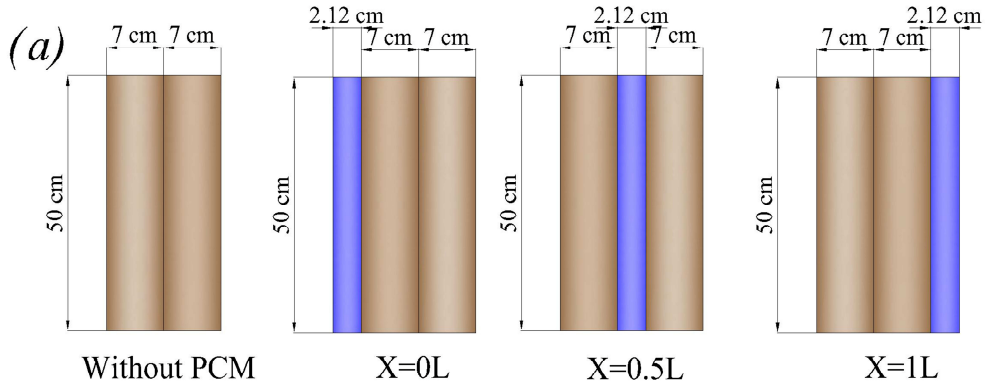

166

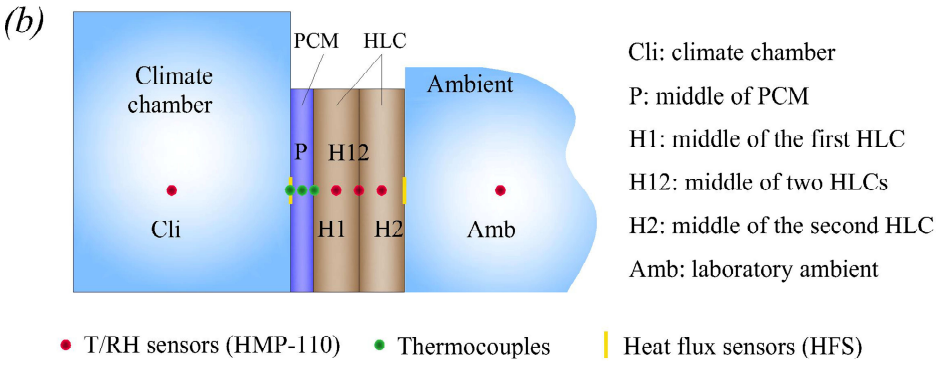

167

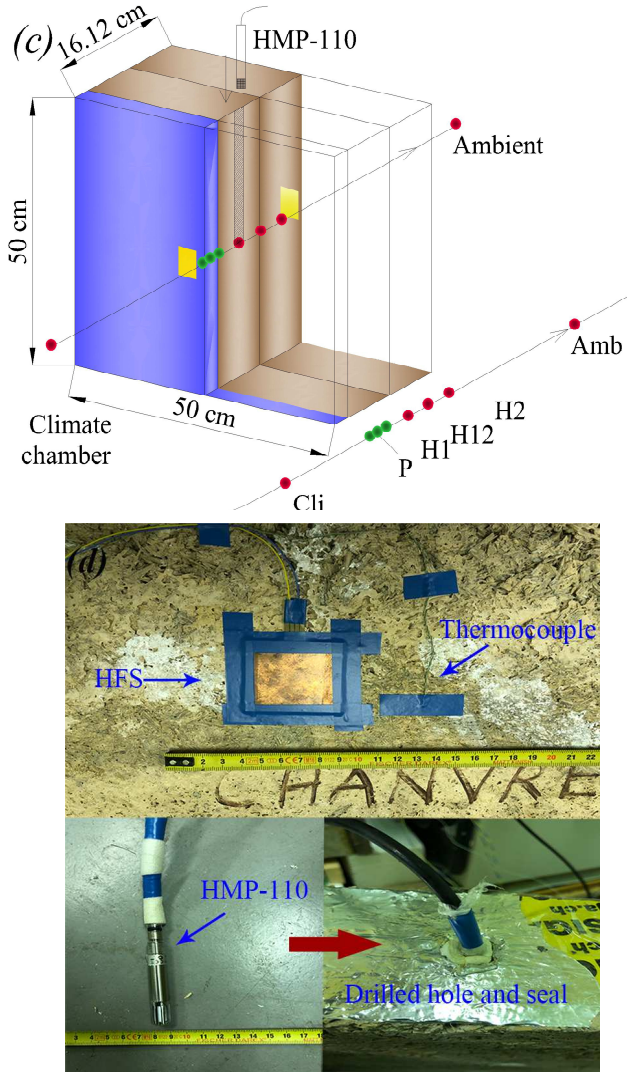

Fig. 4. (a) Four envelope configurations of integrating HLC and PCM; (b) Monitoring points for temperature, relative humidity, and heat flux of configuration X=0 L; (c) 3D view of monitoring points of configuration X=0 L; (d) Different monitoring sensors

Experimental monitoring was ensured by several temperature and relative humidity sensors (HMP-110) that were placed inside the climate chamber, within the laboratory ambient air, and at different positions within the integrated envelope. The HMP-110 sensor is 71 mm long and 12 mm in diameter. They were inserted into each HLC's geometrical center through drilled holes from the lateral side (Fig. 4(c)). Meanwhile, the HMP-110 sensor's cable was sealed by polyethylene film and

179 polystyrene foam, and the hole was sealed by polyvinyl chloride tape, avoiding temperature and
180 humidity interference from cable heat and the ambient hygrothermal environment. In order to help
181 measure the PCM's temperature, three thermocouples (K type with diameters of 0.25 mm) were
182 arranged in the middle and on both sides of the PCM. In addition, two heat flux sensors (HFS) were
183 affixed to the envelope's internal and external surfaces. The HFS sensor is only 50 mm × 50 mm ×
184 0.5 mm (width × length × thickness) in size, each side was sealed and affixed to the envelope's
185 surface with polyvinyl chloride tape to avoid air infiltration that could affect measurement results.
186 The main monitoring points were named according to their position from inside climatic chamber to
187 outside ambient. For example, Fig. 4(b, c) shows the names of monitoring points of configuration
188 X=0 L. All sensors were connected (differential voltage) to a Keithley 2700 data acquisition system,
189 which has a resolution of 6.5-digit (22-bit). On the other side, the Keithley 2700 was connected to a
190 computer to record experimental data with a time step of 120 s. Table 3 details the type,
191 measurement range, and accuracy of apparatus and sensors.
192

Apparatus	Type	Range	Accuracy
Climate chamber	LabEvent L	T: -40-180 ℃	T: ±0.3-1 ℃
	C/64/40/3	RH: 10-95%	RH: ±1-3%
Thermocouple	K type	-70-200 ℃	±0.1 ℃
Temperature/Humidity sensor	HMP-110	T: -40-80 ℃	T: ±0.2 ℃ (0-40 ℃); ±0.4 ℃ (-40-0; 40-80 ℃)
		RH: 0-100%	RH: ±1.5% (0-90%); ±2.5% (90-100%)
Heat flux sensor	HFS	-2000-2000 W/m^2	2%
Data acquisition equipment	Keithley 2700	0.1 μV-1000 V (Voltage)	0.002% (Voltage)

193 Table 3 Apparatus and sensors

2.3. Boundary conditions

The experimental laboratory is a room located in a large building. During experimentation of the four configurations, there were minor fluctuations in temperature and relative humidity. By calculation, the temperature's and relative humidity's mean value and standard deviation (SD) of each configuration and the overall experimental period are shown in Table 4. It can be seen that both temperature and relative humidity have a small SD, indicating a relatively stable hygrothermal environment in the laboratory ambient to imitate indoor conditions.

Configurations	Temperature [℃]	Relative humidity [%]
Without PCM	24.4 ± 0.4	42.4 ± 1.7
X=0 L	26.0 ± 0.4	38.3 ± 3.8
X=0.5 L	27.1 ± 0.8	38.4 ± 3.2
X=1 L	26.3 ± 0.8	41.1 ± 3.9
Overall	25.9 ± 1.5	40.1 ± 3.7

Table 4 Temperature and relative humidity in the laboratory ambient

Therefore, it was essential to ensure appropriate boundary conditions in the climate chamber. Fig. 5(a) shows the temperature and relative humidity changes in the climate chamber in order to imitate outdoor conditions. Before starting, the temperature and relative humidity were set as 15 ℃ and 85% for two days to ensure heat and moisture stabilization in the envelope. Four combinations of temperature and relative humidity changes were then made, including two identical and two opposite

trends, with each combination being kept for one day. The wide temperature and relative humidity range (Fig. 5(b)) provided the dynamic change of boundary conditions and guaranteed clear hygrothermal feedback within the envelope. With this boundary condition, it is possible to analyze measurement results and link the integrated envelope's hygrothermal behavior to the obvious changes in temperature-humidity coupling.

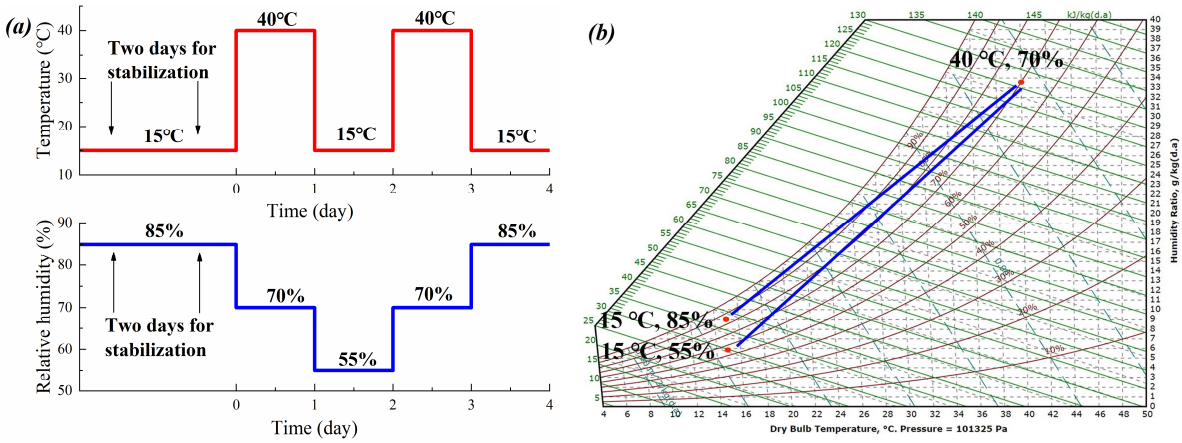

Fig. 5. (a) Boundary temperature and relative humidity condition provided by the climate chamber; (b) Boundary temperature and relative humidity in the psychrometric chart

3. Results and discussion

In this section, the hygrothermal behavior within the HLC envelope of the configuration without PCM (HLC only) is presented first as a reference. Then it is compared to the configurations with PCM. The changes in the overall trend, value, amplitude, and hygrothermal behavior differences between different positions are discussed.

3.1. Hygrothermal behavior of configuration without PCM

Fig. 6 presents the temperature and relative humidity behavior at different monitoring points (see Fig. 4). It can be seen from figure that the temperature remained relatively stable during the 12 hours before the start (0 day) of the experiment. By calculation, the mean value and SD of temperature at points H1, H12, and H2 was 19.25 ± 0.06, 20.60 ± 0.07, and 22.01 ± 0.10 ℃ respectively. Similarly, relative humidity values were 54.29 ± 0.12, 47.07 ± 0.10, and 43.54 ± 0.13%. The small SD indicates that the experimental process started with a hygrothermal equilibrium state.

For temperature, the amplitude applied on the chamber side decreases towards the constant ambient condition over successive layers. The temperature amplitude obtained at points H1, H12, and H2 varied, with values of 8.3, 6.2, and 4.1 ℃ respectively. As regards relative humidity values, there were noticeable differences between the three points. They changed in descending order from the climate chamber to the ambient, i.e., H1 has the highest relative humidity while H2 has the lowest. The amplitude was 6.5, 6.5, and 4% at H1, H12, and H2 respectively. In the following discussion we will keep in mind that moisture transfer is continuous from the climate chamber toward the ambient, whereas the heat transfer changes direction depending on heating and cooling period.

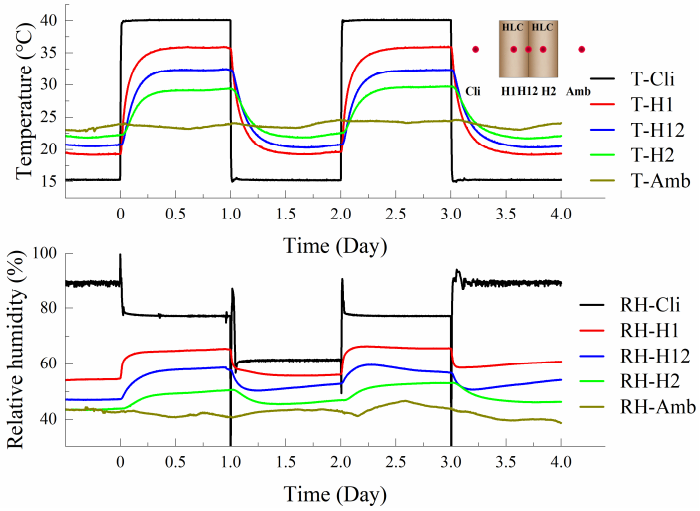

Fig. 6. Temperature and relative humidity behavior of configuration without PCM

As regards the relative humidity trend within the HLC, it underwent two successive decreases followed by two successive increases. It showed the climate chamber's ability to adjust relative humidity quickly and the ambient relative humidity's relative stabilization. The relative humidity change within the HLC was highly consistent with temperature at all times. For example, even though the boundary temperature and relative humidity changed in opposite directions (one increased and the other decreased) on the first and fourth days, the relative humidity trend was still consistent with the temperature. Hence, the relative humidity change was dominated by temperature change. The psychrometric chart (Fig. 5(b)) summarizes this phenomenon: a positive relative humidity difference plus a temperature difference may be equivalent to negative partial pressure. It shows that vapor transfer is the consequence of water vapor pressure, and so a consequence of both temperature and relative humidity differences.

As for the relative humidity on different days and in different positions, it generally obeyed some principles even if there were small differences between them. For example, in most days at H1 and

H12, relative humidity increased/decreased sharply at the beginning of each step because temperature feedback was faster than relative humidity. Therefore, after the sudden temperature change in the climate chamber, the temperature at H1 and H12 also changed sharply. It induced the vapor phase change within HLC because the temperature change induce the evaporation/condensation phenomenon, which led to the increased/decreased relative humidity [24, 25, 53]. As for point H2 away from the climate chamber, feedback to the temperature in the climate chamber was relatively weak and less vapor phase change phenomenon occurred. On the other hand, the relative humidity in the climate chamber also affected the relative humidity within HLC, and the effect was stronger if the position was closer to the climate chamber. For example, at H1, the relative humidity on the second and fourth day suffered from the decrease in temperature. However, after the sharp decrease caused by temperature, it kept decreasing on the second day while started to increase on the fourth day. Because the decrease in relative humidity in the climate chamber on the second day led to evacuation of vapor from the HLC and a decrease in relative humidity within the HLC. Conversely, the increased relative humidity in the climate chamber on the fourth day caused moisture diffusion from the climate chamber to the envelope and increased the relative humidity within the HLC. This phenomenon was not observed at H12, which was farther from the climate chamber than H1 and was less affected. Therefore, the coupling effect between temperature and relative humidity within the HLC was highlighted according to the relative humidity change at H1, and temperature played a dominant role.

To evaluate how quickly temperature and relative humidity change, the characteristic time (τ) was referred to in our study. Characteristic times have been widely used in many fields, including

electrical pollutants, thermal physics, and neuroscience. General time (t) evolution versus characteristic time is expressed as [54]:

$$C_s(t) = C_{s,0} + \Delta C \cdot \exp(-t/\tau)$$

Where C_s is the parameter under study; $C_{s,0}$ is the initial value of parameter under study; and ΔC is the applied difference.

In this study, characteristic time changes from one stable state to the other can quantify the dynamic thermal response under the sudden change in boundary conditions and characterize the material's thermal/hygric inertia. Therefore, the curve fitting of temperature and relative humidity was first conducted according to the formula above, and then the characteristic time was obtained from the fitting result. To simplify the analysis, only the temperature and relative humidity curves at H1, H12, and H2 on the first day were taken into consideration.

By calculation, temperature characteristic times were 7.7×10^3, 8.5×10^3, and 9.9×10^3 s at positions H1, H12, and H2 respectively. The change in value was expected, as was the linear change from the climate chamber to the ambient based on the consecutive thermal resistances of the envelope as it changed the initial value and applied difference. As with relative humidity, characteristic times at H1, H12, and H2 were 1.0×10^4, 1.2×10^4, and 1.6×10^4 s respectively, all higher than the corresponding temperature points. This phenomenon indicated quantitatively that the relative humidity within the HLC requires more time to stabilize than temperature, along with a smoother curve, which was due to the dominant effect of temperature and the HLC's low moisture diffusion.

3.2. Hygrothermal behavior of configurations with PCM

In order to complete the previous section, the effect of combining PCM in three different positions of the envelope was analyzed.

3.2.1. PCM placed on the climate chamber side

The hygrothermal behavior of configuration PCM placed on the climate side (configuration X=0 L) is shown in Fig. 7. Likewise, the SD 12 hours before the start of the experiment was small: 0.07, 0.09, 0.15 ℃ for temperature and 0.23, 0.31, 0.41% for relative humidity at H1, H12, and H2, indicating that the experimental process of this configuration also started with an equilibrium state. It was noted that the PCM was moisture impermeable and there was only heat transfer on the climate chamber side. While for the ambient side, heat and moisture transfer can occur simultaneously.

Unlike the configuration without PCM, the temperature did not reach a stable state at the end of each day. Temperature amplitudes at H1, H12, and H2 were 6.5, 4.4, and 2.6 ℃ respectively, a significant decrease compared to the configuration without PCM. Meanwhile, the temperature difference between the three points was significantly reduced. These phenomena were caused by the existence of PCM, as high PCM thermal inertia was available to prevent the temperature from rising/dropping during the heating/cooling period, i.e., it damped the temperature change and fluctuation.

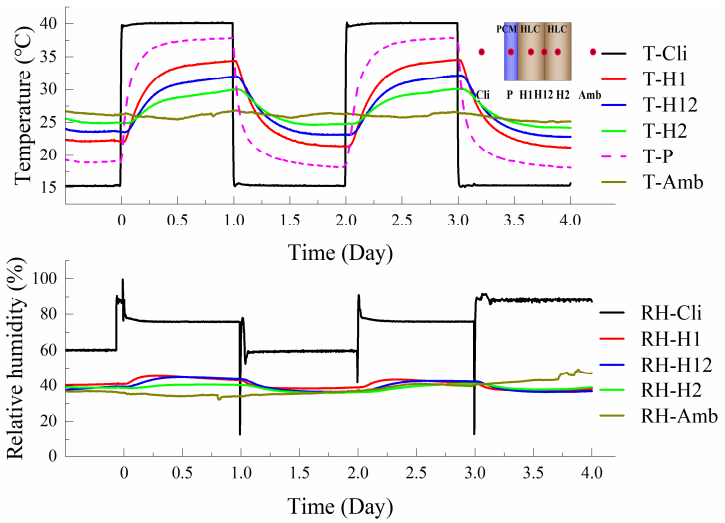

Fig. 7. Temperature and relative humidity behavior of the configuration X=0 L

Focusing on the relative humidity comparison to the configuration without PCM, the overall value (around 40%) of the three positions within HLC was lower, and the three curves almost overlapped, leading to the smaller difference between them. The PCM is impermeable and blocks the moisture transfer between the chamber and the other layers. Such decoupling in moisture will mostly keep the effect of temperature change on the relative humidity. Relative humidity amplitude was then reduced by 50% due to the influence of PCM. Specifically, the PCM thermal inertia weakened the temperature change and affected the characteristic time. The characteristic times at H1, H12, and H2 were 1.5×10^4, 2.0×10^4, and 2.6×10^4 s respectively, which was higher than the configuration without PCM. As discussed previously, the characteristic time of relative humidity was higher than for temperature. So, the characteristic time of relative humidity (1.6×10^4, 2.5×10^4, 4.3×10^4 s for H1, H12, and H2) was high enough to evolve the relative humidity smoothly. Looking at the three points' initial relative humidity, they were also similar due to the PCM's blocking effect. On the other hand, the moisture transfer between ambient and HLC was very slow and small, making the

336 initial relative humidity within the HLC almost the same as the ambient. Consequently, the relative
337 humidity evolved almost based on the initial value and then fluctuated smoothly with small
338 amplitude.

339 It is worth noting that the overall trend of relative humidity was slightly downward, mainly due to
340 the moisture release. On the one hand, the PCM hampered moisture gain from climate chamber to
341 HLC. On the other hand, only a small amount of moisture was released from HLC to the ambient
342 because it was an intercoupling and separated from the chamber change by the impermeable PCM.
343 Therefore, the PCM placed on the climate chamber (outdoor) side damped the temperature and
344 humidity changes, ensuring the effect of thermal and hygric inertia on the indoor environment.

345

346 **3.2.2. PCM placed on the laboratory ambient side**

347 Fig. 8 indicates hygrothermal behavior when the PCM was placed on the laboratory ambient side
348 (configuration X=1 L). As with configuration X=0 L, the temperature evolution did not reach a
349 steady state at the end of each day, and the difference between the three positions was significantly
350 reduced. Compared with the configuration without PCM, the amplitudes were significantly increased
351 with values of 9.2, 7.5, and 5.4 ℃ at H1, H12, and H2 respectively. These phenomena were related
352 to the PCM, which damped the heat loss/gain between HLC and ambient. Meanwhile, the continuous
353 heat transfer between HLC and the climate chamber also increased the temperature amplitude.
354 Therefore, the PCM's barrier effect on heat and humidity fluxes weakened the difference between
355 three points, which can be proven by the higher characteristic time (1.0×10^4, 1.0×10^4, and $1.7 \times$
356 10^4 s at H1, H12, and H2, respectively) compared to the configuration without PCM.

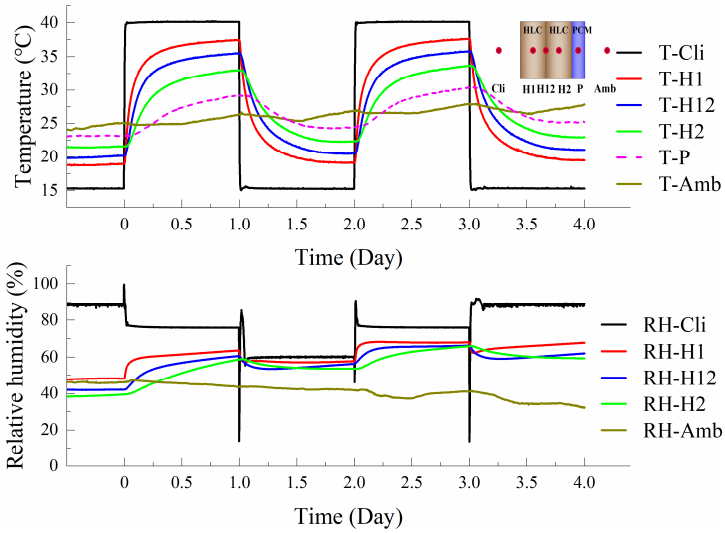

Fig. 8. Temperature and relative humidity behavior of configuration X=1 L

For relative humidity, the curve was relatively smooth and accompanied by small fluctuations as with configuration X=0 L. Nevertheless, the coupling (the change) was more pronounced as the HLC was coupled with the climate chamber and decoupled from the ambient due to the impermeable behavior of PCM on moisture. Compared with the configuration without PCM, the characteristic time for relative humidity was higher (2.6×10^4, 2.2×10^4, and 7.8×10^4 s at H1, H12, and H2 respectively), so lesser differences between each position and smaller amplitude of the curves were observed. It should be noted that although the initial relative humidity between the three positions was closer than with the configuration without PCM, it was a little more incompact compared to configuration X=0 L. Moreover, the initial value at H12 and H2 was close and slightly lower than H1. Since no moisture transferred between HLC and ambient, the initial value at H12 and H2 was mainly affected by the envelope's original relative humidity (around 40%, like X=0 L) and hardly affected by the climate chamber over a short time. In contrast, the initial value at H1 was mainly affected by

373 the climate chamber and consequently higher than the other two points (unidirectional diffusion with
374 impermeable on right side).

375 Likewise, due to the PCM's blocking effect, the moisture accumulation phenomenon occurred
376 within HLC, which made the relative humidity's overall trend an upward trend in order to reach
377 equilibrium between the oscillation within HLC and the average value in the climate chamber.

378

379 **3.2.3. PCM placed in the middle of two HLCs**

380 The previous PCM integration only illustrated one-sided (between the ambient and the HLC or
381 between the climate chamber and the HLC) temperature-humidity coupling. The
382 temperature-humidity coupling between HLC and both sides is discussed in this section for
383 configuration X=0.5 L. The hygrothermal behavior at H1 and H2 of PCM placed in the middle of
384 two HLCs is plotted in Fig. 9. This configuration's main feature was that the temperature and relative
385 humidity difference between H1 and H2 were increased. Taking the end of the first day as an
386 example, the temperature and relative humidity difference between H1 and H2 were 5.9 ℃ and
387 35.3%, higher than the other configurations (temperature difference were 5.8, 4.5, 4.4 ℃ and relative
388 humidity difference were 14.8, 5, 2.7% for the configuration without PCM, X=1 L, and X=0 L
389 respectively). On the one hand, PCM at X=0.5 L damped heat and moisture transfer from one HLC
390 to another. On the other hand, the initial difference and evolution process were also worth noting.
391 The initial temperature and relative humidity differences were large due to the presence of PCM. In
392 addition, temperature and relative humidity evolved smoothly, as was deduced by the characteristic
393 times of temperature and relative humidity (1.2 and 2.4×10^4 s for temperature and 3.6×10^4 and 4.9

394 × 10^4 s for relative humidity at H1 and H2).

395 The relative humidity's slightly upward and downward trend can also be observed. Evolution at
396 H1 had a slight upward trend as with X=1 L while H2 trended downward like X=0 L, caused by
397 moisture accumulation and moisture loss at H1 and H2 respectively.

398

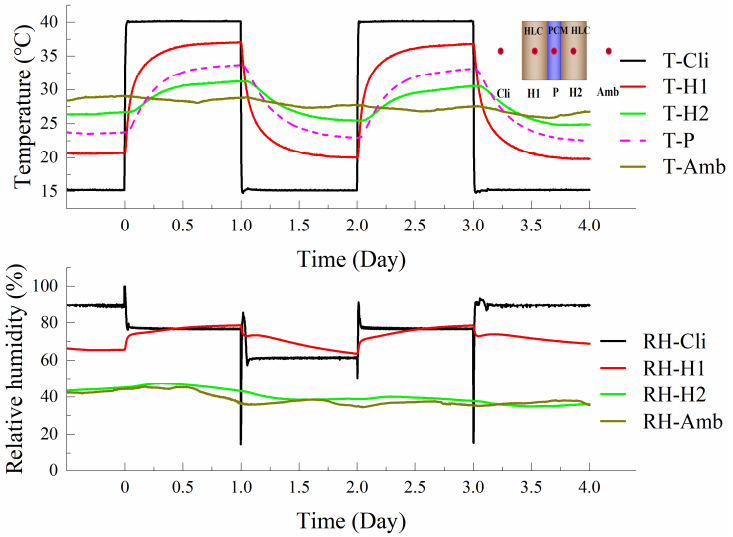

399

400 Fig. 9. Temperature and relative humidity behavior of configuration X=0.5 L

401

402 ## 3.3. Overall hygrothermal comparison

403 To better compare hygrothermal behavior between different configurations, temperature and
404 relative humidity at position H1 of all configurations are compared in Fig. 10(a) and Fig. 10(b)
405 respectively.

406 The temperature and relative humidity in the climate chamber were consistent between all the
407 configurations, which guarantees comparison at the same coordinate. Focusing on the temperature,
408 only the configuration without PCM reached a stable temperature at the end of each day; meanwhile,
409 the amplitude was different between different configurations. The PCM damped the heat transfer

between the climate chamber and HLC (configuration X=0 L), the first HLC and ambient (configuration X=0.5 L/X=1 L), making the amplitude of configuration without PCM (8.3 ℃) higher than X=0 L (6.5 ℃) but lower than X=0.5/0 L (8.5/9.2 ℃). Analyzing the characteristic time, the value of configuration X=0, 0.5, 1 L, and without PCM were 1.5×10^4, 1.2×10^4, 1.0×10^4, and 0.77×10^4 s respectively. This indicated the increase of characteristic time caused by the PCM's participation; the closer the PCM to the climate chamber, the higher the characteristic time.

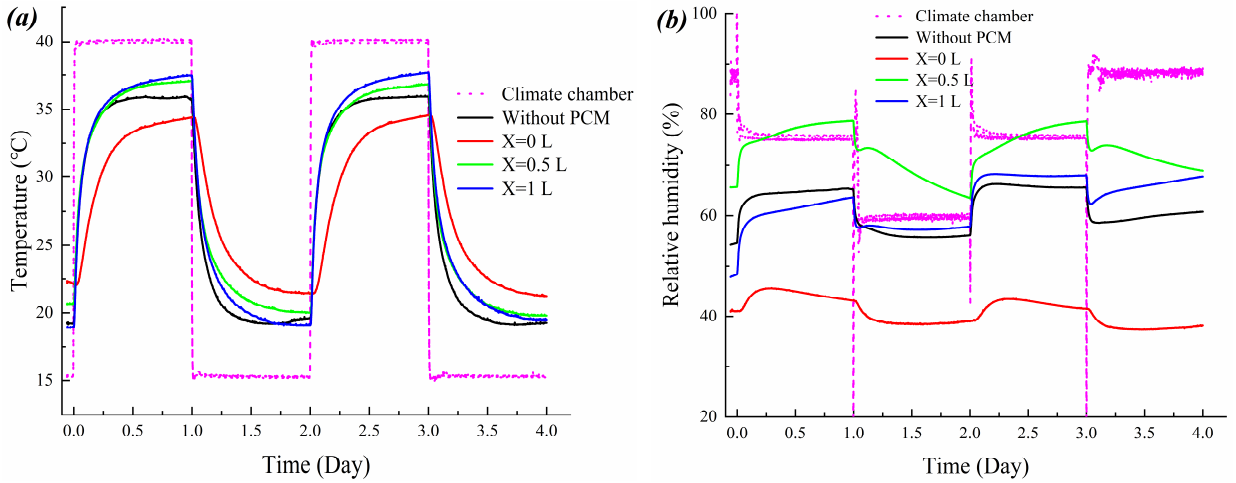

Fig. 10. (a) Temperature and (b) relative humidity behavior at position H1

Relative humidity evolved more smoothly and fluctuated less compared to temperature. Configuration X=0.5 L was the highest and configuration X=0 L the lowest, the other two configurations were in between. This was mainly caused by the initial relative humidity. As mentioned previously, as regards complete moisture transfer block, the initial relative humidity of configuration X=0 L almost equaled the initial relative humidity of the envelope with a low value, whereas the relative humidity of X=0.5 L underwent the relative humidity change from the climate

chamber side but can not transfer to another side, which led to the highest initial relative humidity.

Fig. 11 shows the temperature and relative humidity changes on the first day, which were calculated by the difference between maximum and minimum values. The magnitude order of temperature and relative humidity changes remains consistent, and their values were small when the PCM was close to the climate chamber. The results indicated a high correlation between temperature and relative humidity changes. Moreover, the relative humidity change was reduced with the reduction of temperature change caused by the PCM thermal inertia, which was different depending on the PCM's different positions.

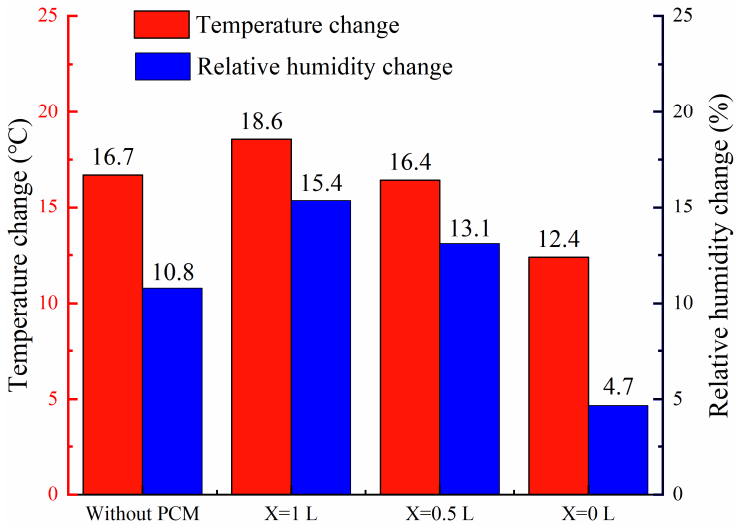

Fig. 11. Temperature and relative humidity change on the first day

3.4. Heat flux and heat store/release capacity

In order to imitate a real building, heat flux and heat store/release were analyzed and calculated. Fig. 12(a) shows the heat flux on the ambient side surface of the envelope; it reflects the heat flux from the ambient side surface (interior envelope surface) to the ambient (indoor environment) after damping by the envelope. The heat flux of PCM configurations was lower than the configuration

without PCM due to its damping effect. Configurations X=0 L and X=0.5 L had a small heat flux fluctuation in the two cycles of heating and cooling period among all the configurations, especially the latter, whose value was almost half of the configuration without PCM. For the heat flux difference between each side of the imitation envelope (Fig. 12(b)). Configurations with PCM had a higher heat flux difference than the configuration without PCM. For configurations with PCM, the heat flux difference of X=0 L was the highest, followed by configurations X=0.5 L and X=1 L. The closer the PCM to the climate chamber, the greater the transient heat flux difference.

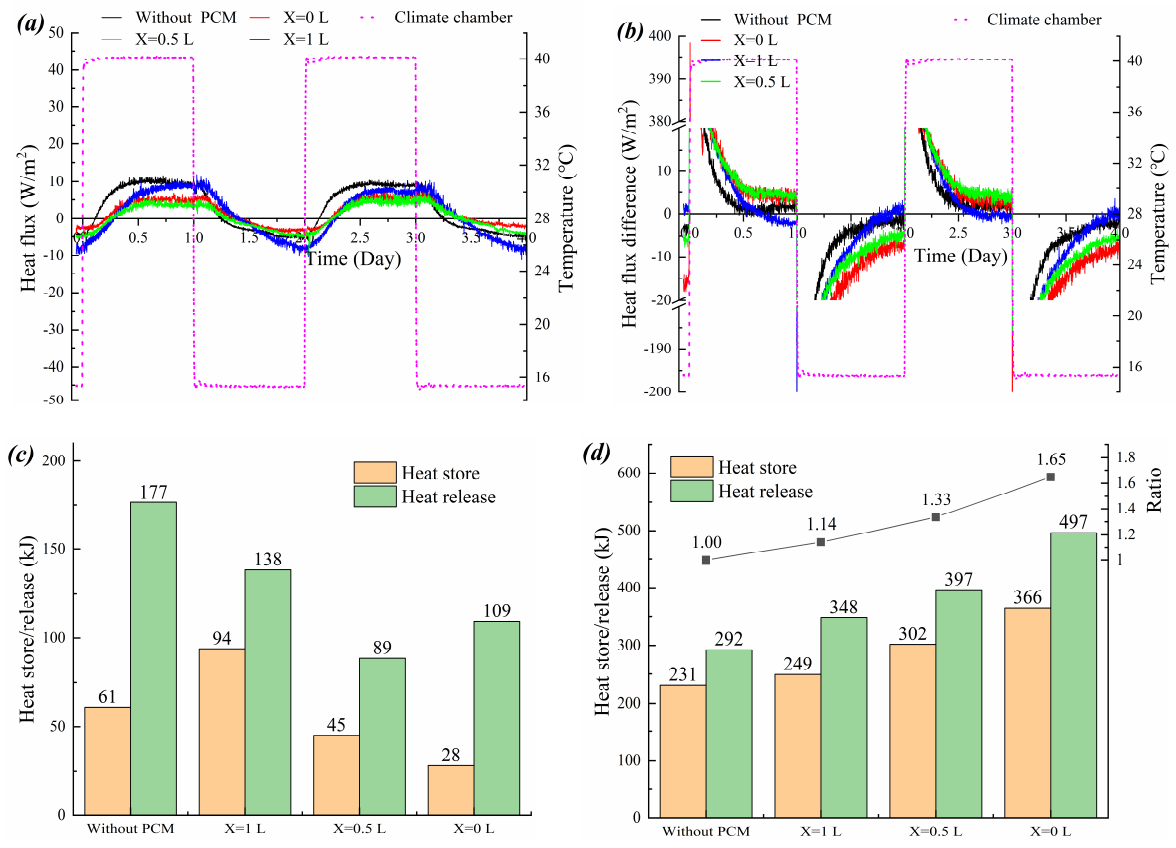

Fig. 12. (a) Heat flux on the ambient side surface of the envelope; (b) Heat flux difference between each side of the envelope and the imposed temperature (right); (c) Heat store/release by ambient side surface; (d) Heat store/release by the envelope and ratio value (right)

455

456 Since the area between heat flux curves and x-axis (time) was the heat store/release, the integral
457 calculation of stored and released energy in the second cycle of thermal charging and discharging
458 (days 3 and 4) was implemented in accordance with the following formula,

459 $$\mathrm{Q} = \int_{t_1}^{t_2} q\, A dt$$

460 Where Q is the stored/released heat, J; t_1, t_2 are the start and end time of calculation, s; q is
461 the heat flux, W/m^2; A is the area of the envelope, m^2; t is time, s.

462 Heat store/release at the ambient side is presented in Fig. 12(c); it imitates the thermal gain/loss
463 between indoor environment and envelope, which is directly proportional to the building's cooling
464 and heating load. The lowest heating load (28 kJ) and cooling load (89 kJ) were produced by
465 configurations X=0 L and X=0.5 L respectively; their corresponding cooling and heating loads were
466 also the smallest among all configurations. Therefore, these two configurations can save energy
467 consumption in a real building.

468 Fig. 12(d) presents the heat store/release capacity of the whole envelope. The capacity of
469 configurations with PCM was stronger than the one without PCM. Configuration X=0 L showed
470 excellent thermal control capacity. It had the highest heat store/ release capacity, with a value nearly
471 1.6/1.7 times greater than the configuration without PCM. In contrast, the heat store/release capacity
472 of configuration X=1 L was the lowest, but still 1.1/1.2 times higher than the configuration without
473 PCM. Therefore, the configuration with less distance between PCM and climate chamber had a
474 higher heat store/release capacity. Moreover, the ordering relationship of heat store/release capacity
475 showed some regularity, which could be deduced from the ratio value (the sum of heat store and

476 release of each configuration divided by the configuration without PCM) on the right axis. The ratio
477 maintained almost linear growth from left to right, indicating the linear relation between PCM's
478 position and heat store/release capacity. From the analysis above, regardless of the heat store/release
479 from the ambient side or the heat store/release capacity of the envelope itself, configurations X=0 L
480 and X=0.5 L both need to be emphasized. In addition, another phenomenon worth mentioning is that
481 the thermal energy released during the cooling period was more than that stored during the heating
482 period.

483 Fig. 13(a) shows the temperature distribution on both sides of PCM, and the 22 ℃ of y-axis
484 corresponds to the starting point of the x-axis. Since 22 ℃ was the temperature at which maximum
485 specific heat capacity was reached, the position closer to the x-axis in the vertical direction had a
486 higher specific heat capacity. Due to the dynamic temperature change, the equivalent specific heat
487 capacity also changes instantaneously. In order to better observe the dynamic characteristics, the
488 transient specific heat capacity based on the middle temperature of PCM on days 3 and 4 is reflected
489 in Fig. 13(b), and is related to the phenomena observed in Fig. 12. At the beginning of the heating
490 period, the temperature gradient and specific heat capacity of X=0 L were the highest, contributing to
491 major heat storage even though it was low in the middle period. And in the last period, the specific
492 heat capacity and temperature gradients were almost the same. This characteristic was more evident
493 during the cooling period because most of the temperature was in the phase change range and had a
494 higher specific heat capacity than the heating period. For X=0 L in particular, the specific heat
495 capacity was much higher than for X=0.5 L and X=1 L most of the time. This explains the heat
496 store/release difference between different configurations and the higher released heat than stored

497 heat.

498

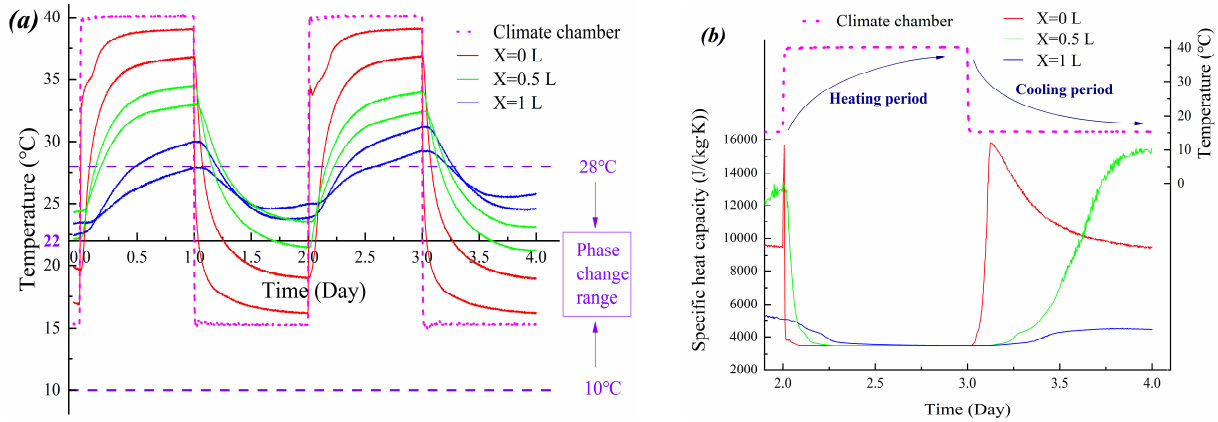

499

500 Fig. 13. (a) Temperature in both side of PCM; (b) Dynamic specific heat capacity of PCM

501

502 ## 4. Conclusion

503 In this paper, the hygrothermal behavior of a new multilayer building envelope integrating HLC
504 and PCM has been studied and analyzed at experimental level. The climate chamber and laboratory
505 ambient imitated outdoor and indoor environments respectively. Four envelope configurations were
506 considered to study the effect of the PCM layer and its positions on the envelope's hygrothermal
507 behavior in terms of the thermal and hygric inertia.

508 The results highlighted the major effect that adding a PCM layer has on the hygrothermal
509 behavior of HLC, characterized by high coupling between temperature and relative humidity
510 variations within the envelope. With inclusion of PCM, characteristic times of temperature and
511 relative humidity both increased, indicating the envelope's increased thermal inertia and hygric
512 inertia. These effects also depend on the PCM's position, although the PCM acts as vapor barrier.

513 When the PCM was placed on the indoor side, the moisture transfer between envelope and

514 indoors was blocked, so hygric inertia was eliminated. Moisture accumulation may occur inside the
515 envelope due to the outdoor environment's high relative humidity. The PCM placed in the middle of
516 the envelope ensures that both sides of the envelope are subject to heat and moisture transfer with the
517 environment. The envelope's hygric inertia was beneficial to the indoor side but the risk of
518 accumulation of humidity on the outdoor side was accentuated. The PCM placed on the outdoor side
519 protected against condensation and mold growth risk caused by the high relative humidity fluctuation.
520 It also ensures that the envelope's hygric inertia has a major effect on the indoor environment.

521 As regards thermal energy behavior, heating and cooling loads were effectively decreased when
522 PCM was placed on the outdoor side and middle of the envelope. In additions, when PCM was
523 placed close to the outdoor side, its heat store/release capacity was enhanced, which was closely
524 related to the PCM's temperature distribution and its corresponding specific heat capacity.

525 Consequently, the PCM placed on the outdoor side was recommended from the perspective of
526 energy savings and envelope hygric inertia. When there is low moisture accumulation risk, PCM in
527 the middle of envelope is also worth considering.

528

529 ## Acknowledgements

530 We thank to the China Scholarship Council (CSC) for its financial support to the first author, No.
531 201808120084. CPER UL/Lorraine Region and PHC Maghreb are acknowledged. The authors
532 would also like to thank EMPP Scientific Pole of the University of Lorraine.

533

Funding

This research did not receive any specific grant from funding agencies in the public, commercial, or not-for-profit sectors.

References

[1] S. Dale, BP Energy Outlook-2019 edition, 2019.
https://www.bp.com/content/dam/bp/business-sites/en/global/corporate/pdfs/energy-economics/energy-outlook/bp-energy-outlook-2019.pdf. (accessed 01 April 2021).
[2] IEA, Energy Efficiency 2017, 2017.
https://www.nrcan.gc.ca/sites/www.nrcan.gc.ca/files/energy/energy-resources/Energy_Efficiency_Marketing_Report_2017.pdf. (accessed 01 April 2021).
[3] IEA, World Energy Outlook 2019, 2019.
https://www.nordicenergy.org/wp-content/uploads/2019/12/6.2_12-Dec_14.00-14.30_WEOslides-for-DT-for-COP25-FINAL.pdf. (accessed 01 April 2021).
[4] M. Bayoumi, Energy saving method for improving thermal comfort and air quality in warm humid climates using isothermal high velocity ventilation, Renewable Energy 114 (2017) 502-512.https://doi.org/10.1016/j.renene.2017.07.056
[5] S. Morsli, A. Sabeur, H. Ramenah, M. El Ganaoui, R. Bennacer, Thermo-Fluid Simulation for Indoor Air Quality and Buildings Thermal Comfort, International Conference on Materials & Energy, EDP Sciences, p. 6.https://doi.org/10.1051/matecconf/202030701032
[6] K. Abe, Assessment of the environmental conditions in a museum storehouse by use of a fungal index, International Biodeterioration & Biodegradation 64(1) (2010) 32-40.https://doi.org/10.1016/j.ibiod.2009.10.004
[7] H.J. Moon, S.H. Ryu, J.T. Kim, The effect of moisture transportation on energy efficiency and IAQ in residential buildings, Energy and Buildings 75 (2014) 439-446.https://doi.org/10.1016/j.enbuild.2014.02.039
[8] A. de Gracia, R. Barzin, C. Fernández, M.M. Farid, L.F. Cabeza, Control strategies comparison of a ventilated facade with PCM – energy savings, cost reduction and CO2 mitigation, Energy and Buildings 130 (2016) 821-828.https://doi.org/10.1016/j.enbuild.2016.09.007
[9] F. Pittau, F. Krause, G. Lumia, G. Habert, Fast-growing bio-based materials as an opportunity for storing carbon in exterior walls, Building and Environment 129 (2018) 117-129.https://doi.org/10.1016/j.buildenv.2017.12.006
[10] F. Scrucca, C. Ingrao, C. Maalouf, T. Moussa, G. Polidori, A. Messineo, C. Arcidiacono, F. Asdrubali, Energy and carbon footprint assessment of production of hemp hurds for application in buildings, Environmental Impact Assessment Review 84 (2020) 106417.https://doi.org/10.1016/j.eiar.2020.106417
[11] M. Rahim, O. Douzane, A.D. Tran Le, G. Promis, T. Langlet, Experimental investigation of hygrothermal behavior of two bio-based building envelopes, Energy and Buildings 139 (2017) 608-615.https://doi.org/10.1016/j.enbuild.2017.01.058
[12] G. Almeida, R. Rémond, P. Perré, Hygroscopic behaviour of lignocellulosic materials: Dataset at oscillating relative humidity variations, Journal of Building Engineering 19 (2018) 320-333.https://doi.org/10.1016/j.jobe.2018.05.005
[13] M. Rahim, O. Douzane, A.D. Tran Le, G. Promis, T. Langlet, Characterization and comparison of hygric properties

of rape straw concrete and hemp concrete, Construction and Building Materials 102 (2016) 679-687.https://doi.org/10.1016/j.conbuildmat.2015.11.021
[14] L. Liu, H. Li, A. Lazzaretto, G. Manente, C. Tong, Q. Liu, N. Li, The development history and prospects of biomass-based insulation materials for buildings, Renewable and Sustainable Energy Reviews 69 (2017) 912-932.https://doi.org/10.1016/j.rser.2016.11.140
[15] G. Costantine, C. Maalouf, T. Moussa, G. Polidori, Experimental and numerical investigations of thermal performance of a Hemp Lime external building insulation, Building and Environment 131 (2018) 140-153.https://doi.org/10.1016/j.buildenv.2017.12.037
[16] M. Rahim, O. Douzane, A.D. Tran Le, T. Langlet, Effect of moisture and temperature on thermal properties of three bio-based materials, Construction and Building Materials 111 (2016) 119-127.https://doi.org/10.1016/j.conbuildmat.2016.02.061
[17] A.D. Tran Le, J.S. Zhang, Z. Liu, D. Samri, T. Langlet, Modeling the similarity and the potential of toluene and moisture buffering capacities of hemp concrete on IAQ and thermal comfort, Building and Environment 188 (2021) 107455.https://doi.org/10.1016/j.buildenv.2020.107455
[18] E. Latif, M. Lawrence, A. Shea, P. Walker, Moisture buffer potential of experimental wall assemblies incorporating formulated hemp-lime, Building and Environment 93 (2015) 199-209.https://doi.org/10.1016/j.buildenv.2015.07.011
[19] M. Rahim, O. Douzane, A.D. Tran Le, G. Promis, B. Laidoudi, A. Crigny, B. Dupre, T. Langlet, Characterization of flax lime and hemp lime concretes: Hygric properties and moisture buffer capacity, Energy and Buildings 88 (2015) 91-99.https://doi.org/10.1016/j.enbuild.2014.11.043
[20] S. Pretot, F. Collet, C. Garnier, Life cycle assessment of a hemp concrete wall: Impact of thickness and coating, Building and Environment 72 (2014) 223-231.https://doi.org/10.1016/j.buildenv.2013.11.010
[21] Y. Florentin, D. Pearlmutter, B. Givoni, E. Gal, A life-cycle energy and carbon analysis of hemp-lime bio-composite building materials, Energy and Buildings 156 (2017) 293-305.https://doi.org/10.1016/j.enbuild.2017.09.097
[22] M. Sinka, D. Bajare, S. Gendelis, A. Jakovics, In-situ measurements of hemp-lime insulation materials for energy efficiency improvement, Energy Procedia 147 (2018) 242-248.https://doi.org/10.1016/j.egypro.2018.07.088
[23] F. Collet, S. Pretot, Experimental highlight of hygrothermal phenomena in hemp concrete wall, Building and Environment 82 (2014) 459-466.https://doi.org/10.1016/j.buildenv.2014.09.018
[24] N. Chennouf, B. Agoudjil, T. Alioua, A. Boudenne, K. Benzarti, Experimental investigation on hygrothermal performance of a bio-based wall made of cement mortar filled with date palm fibers, Energy and Buildings 202 (2019) 109413.https://doi.org/10.1016/j.enbuild.2019.109413
[25] D. Lelievre, T. Colinart, P. Glouannec, Hygrothermal behavior of bio-based building materials including hysteresis effects: Experimental and numerical analyses, Energy and Buildings 84 (2014) 617-627.https://doi.org/10.1016/j.enbuild.2014.09.013
[26] C. Feng, H. Janssen, Hygric properties of porous building materials (II): Analysis of temperature influence, Building and Environment 99 (2016) 107-118.https://doi.org/10.1016/j.buildenv.2016.01.016
[27] S. Poyet, S. Charles, Temperature dependence of the sorption isotherms of cement-based materials: Heat of sorption and Clausius–Clapeyron formula, Cement and Concrete Research 39(11) (2009) 1060-1067.https://doi.org/10.1016/j.cemconres.2009.07.018
[28] T. Colinart, P. Glouannec, Temperature dependence of sorption isotherm of hygroscopic building materials. Part 1: Experimental evidence and modeling, Energy and Buildings 139 (2017) 360-370.https://doi.org/10.1016/j.enbuild.2016.12.082
[29] T. Colinart, P. Glouannec, M. Bendouma, P. Chauvelon, Temperature dependence of sorption isotherm of

hygroscopic building materials. Part 2: Influence on hygrothermal behavior of hemp concrete, Energy and Buildings 152 (2017) 42-51.https://doi.org/10.1016/j.enbuild.2017.07.016
[30] M. Rahim, A.D. Tran Le, O. Douzane, G. Promis, T. Langlet, Numerical investigation of the effect of non-isotherme sorption characteristics on hygrothermal behavior of two bio-based building walls, Journal of Building Engineering 7 (2016) 263-272.https://doi.org/10.1016/j.jobe.2016.07.003
[31] N. Chennouf, B. Agoudjil, A. Boudenne, K. Benzarti, F. Bouras, Hygrothermal characterization of a new bio-based construction material: Concrete reinforced with date palm fibers, Construction and Building Materials 192 (2018) 348-356.https://doi.org/10.1016/j.conbuildmat.2018.10.089
[32] M. El Ganaoui, J. Hristov, M. Lacroix, Analytical and innovative solutions for heat transfer problems involving phase change and interfaces, Comptes Rendus Mécanique 340(7) (2012) 463-465.https://doi.org/10.1016/j.crme.2012.04.002
[33] J. Yu, K. Leng, H. Ye, X. Xu, Y. Luo, J. Wang, X. Yang, Q. Yang, W. Gang, Study on thermal insulation characteristics and optimized design of pipe-embedded ventilation roof with outer-layer shape-stabilized PCM in different climate zones, Renewable Energy 147 (2020) 1609-1622.https://doi.org/10.1016/j.renene.2019.09.115
[34] Y. Kharbouch, A. Mimet, M. El Ganaoui, L. Ouhsaine, Thermal energy and economic analysis of a PCM-enhanced household envelope considering different climate zones in Morocco, International Journal of Sustainable Energy 37(6) (2018) 515-532.https://doi.org/10.1080/14786451.2017.1365076
[35] A. Laaouatni, N. Martaj, R. Bennacer, M. Lachi, M. El Omari, M. El Ganaoui, Thermal building control using active ventilated block integrating phase change material, Energy and Buildings 187 (2019) 50-63.https://doi.org/10.1016/j.enbuild.2019.01.024
[36] R. Moreau, M. El Ganaoui, R. Prud'homme, Melting and solidification: processes and models/Fusion et solidification : procédés et modèles, Comptes Rendus Mécanique 335(5) (2007) 247-250.https://doi.org/10.1016/j.crme.2007.05.007
[37] P.K.S. Rathore, S.K. Shukla, Potential of macroencapsulated PCM for thermal energy storage in buildings: A comprehensive review, Construction and Building Materials 225 (2019) 723-744.https://doi.org/10.1016/j.conbuildmat.2019.07.221
[38] L. Bin, W. Meixia, W. Qi, M. Shaoli, R. Bennacer, Effect of the Position of the Phase Change Material (PCM Na2CO3•10H2O) on the Solar Chimney Effect, Energy Procedia 139 (2017) 462-467.https://doi.org/10.1016/j.egypro.2017.11.238
[39] Z.X. Li, A.A.A.A. Al-Rashed, M. Rostamzadeh, R. Kalbasi, A. Shahsavar, M. Afrand, Heat transfer reduction in buildings by embedding phase change material in multi-layer walls: Effects of repositioning, thermophysical properties and thickness of PCM, Energy Conversion and Management 195 (2019) 43-56.https://doi.org/10.1016/j.enconman.2019.04.075
[40] S.A. Memon, Phase change materials integrated in building walls: A state of the art review, Renewable and Sustainable Energy Reviews 31 (2014) 870-906.https://doi.org/10.1016/j.rser.2013.12.042
[41] X. Jin, S. Zhang, X. Xu, X. Zhang, Effects of PCM state on its phase change performance and the thermal performance of building walls, Building and Environment 81 (2014) 334-339.https://doi.org/10.1016/j.buildenv.2014.07.012
[42] X. Jin, M.A. Medina, X. Zhang, Numerical analysis for the optimal location of a thin PCM layer in frame walls, Applied Thermal Engineering 103 (2016) 1057-1063.https://doi.org/10.1016/j.applthermaleng.2016.04.056
[43] X. Jin, M.A. Medina, X. Zhang, On the importance of the location of PCMs in building walls for enhanced thermal performance, Applied Energy 106 (2013) 72-78.https://doi.org/10.1016/j.apenergy.2012.12.079

[44] X. Jin, D. Shi, M.A. Medina, X. Shi, X. Zhou, X. Zhang, Optimal location of PCM layer in building walls under Nanjing (China) weather conditions, Journal of Thermal Analysis and Calorimetry 129(3) (2017) 1767-1778.https://doi.org/10.1007/s10973-017-6307-3
[45] K.O. Lee, M.A. Medina, E. Raith, X. Sun, Assessing the integration of a thin phase change material (PCM) layer in a residential building wall for heat transfer reduction and management, Applied Energy 137 (2015) 699-706.https://doi.org/10.1016/j.apenergy.2014.09.003
[46] A. Lagou, A. Kylili, J. Šadauskienė, P.A. Fokaides, Numerical investigation of phase change materials (PCM) optimal melting properties and position in building elements under diverse conditions, Construction and Building Materials 225 (2019) 452-464.https://doi.org/10.1016/j.conbuildmat.2019.07.199
[47] A. Fateh, F. Klinker, M. Brütting, H. Weinläder, F. Devia, Numerical and experimental investigation of an insulation layer with phase change materials (PCMs), Energy and Buildings 153 (2017) 231-240.https://doi.org/10.1016/j.enbuild.2017.08.007
[48] A. Fateh, D. Borelli, F. Devia, H. Weinläder, Summer thermal performances of PCM-integrated insulation layers for light-weight building walls: Effect of orientation and melting point temperature, Thermal Science and Engineering Progress 6 (2018) 361-369.https://doi.org/10.1016/j.tsep.2017.12.012
[49] R.A. Kishore, M.V.A. Bianchi, C. Booten, J. Vidal, R. Jackson, Parametric and sensitivity analysis of a PCM-integrated wall for optimal thermal load modulation in lightweight buildings, Applied Thermal Engineering 187 (2021) 116568.https://doi.org/10.1016/j.applthermaleng.2021.116568
[50] R.A. Kishore, M.V.A. Bianchi, C. Booten, J. Vidal, R. Jackson, Optimizing PCM-integrated walls for potential energy savings in U.S. Buildings, Energy and Buildings 226 (2020) 110355.https://doi.org/10.1016/j.enbuild.2020.110355
[51] M.P. Sáez-Pérez, M. Brümmer, J.A. Durán-Suárez, A review of the factors affecting the properties and performance of hemp aggregate concretes, Journal of Building Engineering 31 (2020) 101323.https://doi.org/10.1016/j.jobe.2020.101323
[52] D. Energain®, Hydrocarbon-based PCM Applications, 2010. https://cdn2.hubspot.net/hub/55819/file-14755587-pdf/docs/buildings-xi/dupont_energain.pdf. (accessed 01 March 2021).
[53] Y. Aït Oumeziane, S. Moissette, M. Bart, F. Collet, S. Pretot, C. Lanos, Influence of hysteresis on the transient hygrothermal response of a hemp concrete wall, Journal of Building Performance Simulation 10(3) (2017) 256-271.https://doi.org/10.1080/19401493.2016.1216166
[54] R.W. Lewis, P. Nithiarasu, K.N. Seetharamu, Fundamentals of the finite element method for heat and fluid flow, John Wiley & Sons2004.https://doi.org/10.1002/0470014164